Acid-sensing ion channels ASIC2 and ASIC3 do not contribute to mechanically activated currents in mammalian sensory neurones

Liam J. Drew[1], Daniel K. Rohrer[2], Margaret P. Price[3], Karen E. Blaver[1], Debra A. Cockayne[2], Paolo Cesare [1] and John N. Wood[1]

[1] *Molecular Nociception Group, Department of Biology, University College London, Gower Street, London WC1E 6BT, UK*
[2] *Department of Molecular Pharmacology, Roche Bioscience, Palo Alto, CA, USA*
[3] *Howard Hughes Medical Institute, Roy J and Lucille A. Carver College of Medicine, Iowa City, IA 52242, USA*

The molecular basis of mechanosensory transduction by primary sensory neurones remains poorly understood. Amongst candidate transducer molecules are members of the acid-sensing ion channel (ASIC) family; nerve fibre recordings have shown ASIC2 and ASIC3 null mutants have aberrant responses to suprathreshold mechanical stimuli. Using the neuronal cell body as a model of the sensory terminal we investigated if ASIC2 or 3 contributed to mechanically activated currents in dorsal root ganglion (DRG) neurones. We cultured neurones from ASIC2 and ASIC3 null mutants and compared response properties with those of wild-type controls. Neuronal subpopulations [categorized by cell size, action potential duration and isolectin B4 (IB4) binding] generated distinct responses to mechanical stimulation consistent with their predicted *in vivo* phenotypes. In particular, there was a striking relationship between action potential duration and mechanosensitivity as has been observed *in vivo*. Putative low threshold mechanoreceptors exhibited rapidly adapting mechanically activated currents. Conversely, when nociceptors responded they displayed slowly or intermediately adapting currents that were smaller in amplitude than responses of low threshold mechanoreceptor neurones. No differences in current amplitude or kinetics were found between ASIC2 and/or ASIC3 null mutants and controls. Ruthenium red (5 μM) blocked mechanically activated currents in a voltage-dependent manner, with equal efficacy in wild-type and knockout animals. Analysis of proton-gated currents revealed that in wild-type and ASIC2/3 double knockout mice the majority of putative low threshold mechanoreceptors did not exhibit ASIC-like currents but exhibited a persistent current in response to low pH. Our findings are consistent with another ion channel type being important in DRG mechanotransduction.

(Received 26 November 2003; accepted after revision 21 February 2004; first published online 27 February 2004)
Corresponding author J. N. Wood: Molecular Nociception Group, Department of Biology, UCL, Gower Street, London WC1E 6BT, UK. Email: j.wood@ucl.ac.uk

Mechanosensory transduction by dorsal root ganglion (DRG) neurones is likely to be mediated by pressure directly activating mechanosensitive ion channels (Lewin & Stucky, 2000). However, little is known of the molecular mechanisms that underlie this form of transduction (Gillespie & Walker, 2001).

In *Caenorhabditis elegans* two degenerin/epithelial sodium channel (DEG/ENaC) ion channel subunits, MEC-4 and MEC-10, are required for sensing light touch. These subunits, with MEC-6, putatively form an ion channel within a mechanotransduction complex including intra- and extracellular binding proteins (Tavernarakis & Driscoll, 1997; Ernstrom & Chalfie, 2002). Mammalian acid-sensing ion channels (ASICs) are members of the same superfamily as MEC-4 and MEC-10 and are highly expressed in sensory neurones (Waldmann & Lazdunski, 1998). Consistent with a function in mechanosensation, ASIC2 (Price *et al.* 2000; Garcia-Añoveros *et al.* 2001) and ASIC3 (Price *et al.* 2001) immunoreactivity is detectable in peripheral mechanosensory structures.

Price *et al.* (2000, 2001) ablated the genes for ASIC2 and ASIC3 to investigate their function in somatosensory

 DOI: 10.1113/jphysiol.2003.058693

physiology. Using the skin–nerve preparation, certain classes of sensory axons in null mutants were shown to have aberrant response properties. In ASIC2 knockouts mechanically evoked firing rates of rapidly adapting, and to a lesser degree slowly adapting, Aβ-mechanoreceptors were lower than wild-type responses. In ASIC3 knockouts changes were observed in three modalities. In response to mechanical stimulation, Aδ-nociceptors showed reduced firing frequencies and increased activation thresholds, whereas rapidly adapting mechanoreceptors exhibited increased firing. In C-fibres, responses to pH 5 and noxious heat were both reduced. These data thus suggest a role for ASICs in sensory transduction; however, no direct evidence has been presented demonstrating mechanical activation of ASICs.

Genetic screens have also revealed members of the transient receptor potential (TRP) channel family to be candidate mechanotransducers. Fruit flies lacking the TRP channel NompC showed a substantial loss of movement-evoked receptor potential in bristle mechanoreceptors (Walker *et al.* 2000) and NompC is also essential for zebrafish hearing (Sidi *et al.* 2003). Recently, Kim *et al.* (2003) showed that Nanchung, a TRP-related protein, is expressed exclusively in chordotonal neurones in *Drosophila* and is required for mechanosensation by these cells. Another family member, OSM-9, is required for detection of touch, osmolarity and olfactory stimuli in *C. elegans* (Colbert *et al.* 1997). The closest mammalian homologue of OSM-9, TRPV4, is activated by hypotonicity (Liedtke *et al.* 2000; Strotmann *et al.* 2000) and a recent report (Suzuki *et al.* 2003) suggests animals lacking this channel have diminished pressure sensation in electrophysiological and behavioural assays.

Another approach to studying sensory transduction is to apply physical stimuli to cultured DRG neurones (for examples see Cesare & McNaughton, 1996; Reid *et al.* 2002). We previously characterized the responses of cultured neonatal rat neurones to mechanical stimulation (Drew *et al.* 2002) and showed that categorizing neurones according to their capsaicin sensitivity indicated that they retain aspects of their *in vivo* mechanosensitive phenotypes. In this study we mechanically stimulated cultured adult mouse DRG neurones and investigated the effect of ASIC2 and/or ASIC3 gene ablation on evoked responses.

Methods

All experimental procedures were carried out according to the UK Animals (Scientific Procedures) Act 1986.

Generation of ASIC2 and ASIC3 null mutants

The ASIC2 null mutants used in this study have previously been described in Price *et al.* (2000). Briefly, a neo cassette was inserted into the ASIC2 gene to replace two exons encoding the entire second transmembrane domain and part of the putative pore-forming domain.

Genetic disruption of the mouse ASIC3 gene was carried out by a standard positive–negative selection scheme (Mansour *et al.* 1988) in mouse R1 embryonic stem cells (Nagy *et al.* 1993). The targeting vector contained a 2.3 kb *Hin*d 3/*Nsi* I 5′-arm of homology (−2211 to +83 base pairs relative to the initiator ATG codon) and a 6.2 kb *Sph* I/*Sph* I 3′-arm of homology (+1880 to +8083 relative to ATG), flanking the thymidine kinase (TK)-neo positive selection cassette (Fig. 1*A*). This led to the deletion of the first two coding exons (containing amino acids 28–229). Speed Congenics (Jackson Laboratories, Bar Harbour, ME, USA; see http://jaxmice.jax.org/library/communication/communication06.pdf) was applied to ASIC3 gene-targeted mice, utilizing C57Bl/6J mice as the backcross strain. ASIC3 heterozygous null mice, determined to be genetically >99% C57Bl/6J by marker-assisted backcrossing, were then intercrossed to generate ASIC3 homozygous null mice.

In both cases experimental animals were the offspring of matings of either knockout (KO) or wild-type pairings from the offspring of heterozygous parents. To generate mice lacking both genes ASIC2 nulls were bred to ASIC3 nulls to generate animals heterozygous for both genes. These animals were then crossed and double KOs and wild-type offspring were selected from the resultant offspring to breed lines of wild-type and double KO mice. Therefore, in all experiments wild-type and KO mice were 'first cousins'.

ASIC3 expression studies

Total RNA was isolated using the Trizol reagent (Invitrogen, Carlsbad, CA, USA). Two mice were used for each tissue tested, with the exception of dorsal root ganglia, which, owing to their small size, were pooled for sufficient RNA template. Reverse transcriptase-polymerase chain reaction (RT-PCR) amplification of ASIC3 mRNA was done using 1 μg of total RNA in the Supercript One Step RT-PCR system (Invitrogen). Glyceraldehyde phosphate dehydrogenase (GAPDH) was used as an internal standard. RT-PCR was carried out under the following thermal cycling conditions: 50°C, 30 min; followed by 94°C, 3 min. This first step was then followed by 30 cycles of 94°C, 30 s; 60°C, 1 min; 72°C, 2.5 min; and a final extension step of 72°C, 10 min. Primer sequences spanned exon–

intron boundaries so that products of the expected size could only be derived from properly spliced mRNA templates. Primer sequences used for RT-PCR were as follows:

ASIC3 sense primer, 5′ATGAAACCTCCCTCAGG ACTGGAG-3′
ASIC3 antisense primer, 5′-TTCCTCCTGGCCGTGG ATCTGCAC-3′
Expected amplicon, 741 bp
GAPDH sense primer, 5′-TCAACGACCCCTTGATTGA CC-3′
GAPDH antisense primer, 5′-GGATGCAGGGATGATG TTCTGG-3′
Expected amplicon, 534 bp.

Products were electrophoresed on 1% agarose gels stained with ethidium bromide, and photographed. Gels were then subjected to Southern blot transfer, and ^{32}P-labelled probes specific for ASIC3 and GAPDH were used to verify the amplification products.

Cell culture

Cells were cultured from adult mice (ASIC2 and ASIC2/3 KOs: 6–9 weeks, ASIC3 KOs: 14–16 weeks). Animals were killed by inhalation of a rising concentration of CO_2 followed by cervical dislocation and 20–25 dorsal root ganglia were dissected from each. Ganglia were digested in collagenase (Type XI, 0.6 mg ml^{-1}, reagents from Sigma unless stated otherwise), dispase (3.0 mg ml^{-1}) and glucose (1.8 mg ml^{-1}) in Ca^{2+},Mg^{2+}-free PBS for 40 min prior to mechanical trituration. Cells were then resuspended in Dulbecco's modified Eagle's medium (DMEM) containing 10% fetal bovine serum (Gibco), 2 mM glutamine (Gibco), 10 000 i.u. ml^{-1} penicillin–streptomycin (Gibco) and 100 ng ml^{-1} nerve growth factor (NGF) and plated on 35 mm dishes coated with poly-L-lysine and laminin. Recordings were made 16–36 h after plating.

Electrophysiology and solutions

Neurones whose soma was not in contact with those of other neurones were selected for recording. Whole-cell, perforated patch recordings were made using an Axopatch 200B amplifier (Axon Instruments) controlled by pCLAMP 6 (Axon Instruments). Data was acquired at 5–20 kHz. Patch pipettes were made from thin-walled glass (Harvard Apparatus) and had an initial resistance of 2–3 MΩ when filled with internal solution. Seals had a series resistance of 4–10 MΩ, compensated for by 40–60% (feedback lag; 15 μs) in both voltage- and current-clamp experiments. Voltage-clamp recordings were made at a holding potential of –70 mV unless otherwise stated. For cell-to-cell comparison action potential recordings in

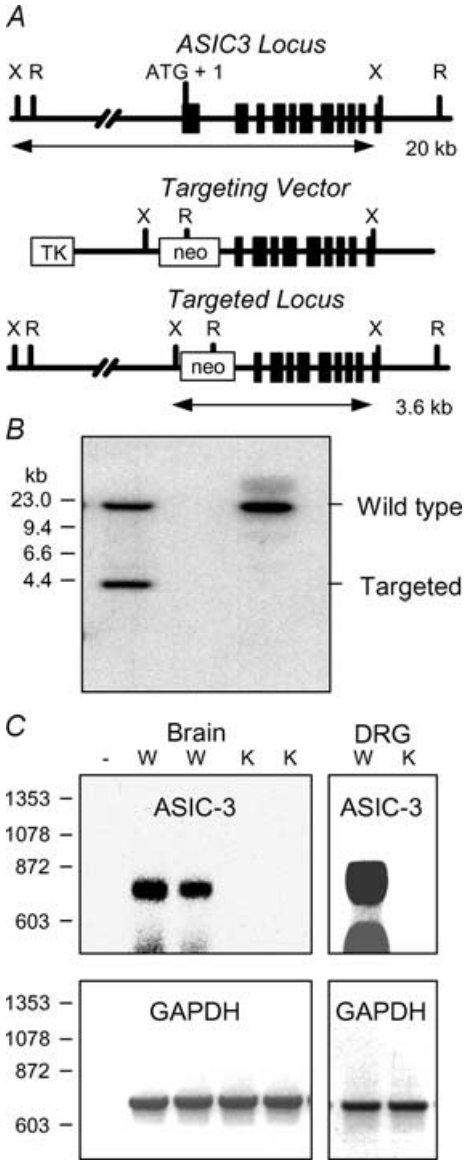

Figure 1. Disruption of the ASIC3 gene in mice
A, the wild-type ASIC3 gene has 11 identified exons (rectangles). The wild-type ASIC3 locus is bounded by two *Xba* I sites, ~20 kb apart (X = *Xba* I, R = *Eco*R I). The middle panel shows the ASIC3 gene targeting vector that deletes most of exon 1 and all of exon 2. Targeted constructs acquired a new *Xba* I site, 3.6 kb upstream from the endogenous 3′ *Xba* I site. *B*, Southern blot analysis of ASIC3 gene-targeted embryonic stem cells. Wild-type and gene-targeted fragment sizes are indicated. *C*, RT-PCR analysis of mRNA expression in wild-type and ASIC3 null mice. Separate reactions were carried out for GAPDH and ASIC3, under identical amplification conditions. Amplification products were electrophoresed, Southern blotted, and probed with ^{32}P cDNA probes. W = wild-type, K = ASIC3 null, – = no RNA.

the current-clamp configuration were made from a baseline potential of −70 mV, adjusted by passing polarizing current.

Standard intracellular solution contained (mM): 110 methanesulphonic acid, 30 KCl (BDH), 1 $MgCl_2$ and 10 Hepes, pH 7.35 (pH was corrected using KOH; final K^+ concentration ∼140 mM); 200 μg ml^{-1} amphotericin B was added immediately before recording. When testing the blocking efficiency of ruthenium red on inward and outward currents a Cs^+-based internal solution was used (mM): 110 $CsMetSO_4$, 30 CsCl, 1 $MgCl_2$, 10 Hepes, pH 7.3 (adjusted using CsOH). The standard external solution contained (mM): 140 NaCl (BDH), 4 KCl (BDH), 2 $CaCl_2$ (BDH), 1 $MgCl_2$ and 10 Hepes, pH 7.4 (adjusted using NaOH). pH 5.3 solution was made with 10 mM Mes in place of Hepes. Capsaicin was dissolved as a 10 mM stock in DMSO and then diluted in standard external solution to 1 μM. A 500 μM stock solution of ruthenium red was made in external solution. IB4 labelling was achieved by incubating the cells in 3 μg ml^{-1} IB4-Alexa 488 (Molecular Probes) in standard external solution for 10 min and then washing twice in external solution prior to recording.

Mechanical stimulation and drug application

Following seal formation, a series of incrementing mechanical stimuli were applied to the neurone in voltage clamp. The recording configuration was then switched to current clamp and a series of incrementing, depolarizing currents were passed to elicit action potentials. Working with adult animals allowed us to use action potential properties to divide neurones into presumptive low and high threshold mechanoreceptor populations as membrane properties of sensory neurones reach a mature state after postnatal week 3 (Fitzgerald & Fulton, 1992). Subsequently, in voltage clamp the presence or absence of tetrodotoxin-resistant (TTX-r) voltage-activated sodium currents was noted and the characteristics of the celal's responses to protons and capsaicin were determined.

Mechanical stimulation of neuronal somata was achieved using a heat-polished glass pipette (tip diameter 5 μm), controlled by a piezo-electric crystal drive (Burleigh), positioned at an angle of 70 deg to the surface of the dish. The probe was positioned so that a 10 μm movement did not visibly contact the cell but that a 12 μm stimulus produced an observable membrane deflection. A 12 μm movement was then defined as a 2 μm stimulation, 14 μm as a 4 μm stimulus, and so on. The probe was moved at a speed of 0.5 μm ms^{-1} and the stimulus was applied for 200 ms. To assess the mechanical sensitivity of a neurone, a series of mechanical steps in 2 μm increments were applied (9 for large cells and 7 for small–medium cells) at 15 s intervals, which was sufficient for full current recovery. Action potentials were evoked by 1 ms (20 ms for ASIC2 mice) square waves of current injection. TTX-r Na^+ currents were tested for by applying a family of 10 ms depolarizing voltage steps whilst the neurone was perfused in 300 nM TTX. Capsaicin (1 μM) and low pH (pH 5.3) were applied for 4 s using a multibarrel rapid solution changer (Biologic). Ruthenium red was applied through a single tube with multiple inputs perfusing the neurone. For these experiments, cells that showed a reproducible response to mechanical stimuli (> 200 pA stimulated, stimulus duration 100 ms, at 20 s intervals) were selected for further experimentation.

Neurone diameters were determined as the mean of the shortest and longest 'diameters' measured using imaging software (Openlab). Action potential amplitude was measured from the baseline potential (−70 mV) to the peak potential change and the duration was measured as the width of the action potential at half the peak amplitude. For analysis of adaptation kinetics, exponentials were only fitted to currents over 150 pA. Data are presented as mean ± S.E.M.

Results

Generation of ASIC3 null mutants

ASIC3 null mutants were generated by using homologous recombination to delete amino acids 28–229 of the ASIC3 genes. This corresponds to removal of the majority of exon 1 and the whole of exon 2 which encode approximately the last third of the amino terminus, the first transmembrane domain and nearly half of the extracellular loop.

Using RT-PCR, ASIC3 mRNA was detected in brain, spinal cord and dorsal root ganglia of wild-type animals but was absent from null mutants (Fig. 1*C*). ASIC3 nulls were indistinguishable from wild-type littermates in terms of gross morphology, behaviour and fertility.

Mechanically activated currents in large, wild-type DRG neurones

As shown previously (McCarter *et al.* 1999; Drew *et al.* 2002) cultured sensory neurones responded to focal mechanical stimulation of their somata with an inward, cationic current. Overall, 70.2% (66/94) of large wild-type neurones (> 35 μm, mean 41.05 ± 0.29 μm) displayed mechanically activated (MA) currents. To determine if the properties of the MA currents correlated with other aspects

of neuronal phenotype we divided the neurones into subpopulations.

We classified neurones according to diameter, action potential properties and IB4 binding and also applied a low pH stimulus (pH 5.3) and capsaicin (1 μM) to each and tested for the presence or absence of TTX-r voltage-activated sodium currents. Others have described a robust correlation between action potential properties and the peripheral receptor type of DRG neurones: low threshold mechanoreceptors have narrow, uninflected action potentials and high threshold mechanoreceptors and nociceptors have wide, inflected action potentials (Koerber *et al.* 1988; Ritter & Mendell, 1992; Lawson, 2002). Therefore, we divided large neurones into those with action potential durations of less than or equal to 1 ms (narrow action potentials) and those with longer action potentials (wide action potentials). The majority of narrow action potentials had uninflected falling phases although some had very minor inflections whereas all wide action potentials showed prominent inflections during repolarization (Fig. 2*A*). This was strongly correlated with the expression of TTX-r sodium currents; only 6.2% (2/32) of narrow action potential neurones expressed TTX-r currents while these currents were present in 97.9% (47/48) of neurones with wide action potentials.

Amongst large DRG neurones from wild-type animals we found a clear distinction between MA currents expressed by narrow and wide action potential neurones (Fig. 2*B*). Of neurones with narrow action potentials, 96.5% (55/57) expressed MA currents and of these 96.4% (53/55) responded to mechanical stimulation with rapidly adapting (RA) currents (Fig. 2*C*). The other two neurones that responded exhibited currents with significantly slower adaptation kinetics. Of the two neurones with action potentials that expressed TTX-r sodium currents one was unresponsive and one had more slowly adapting MA currents.

In contrast, in neurones with wide action potentials, MA currents were only seen in 29.7% (11/37) of cells (χ^2; $P < 0.001$) (Fig. 2*B*). Moreover, the neurones that responded displayed MA currents with distinctly slower adaptation kinetics than those seen in narrow action potential neurones (Fig. 2*C*) and that were much smaller in amplitude (Fig. 2*D*) (2-way, repeated measures ANOVA; $P = 0.02$). The mean maximal response of narrow action potential neurones was 1.57 ± 0.21 nA compared to 0.37 ± 0.17 nA by wide action potential cells. Typical rapidly adapting MA currents in neurones with narrow action potentials were unaffected by exposure to 300 nM TTX; currents in TTX were 99.1 ± 1.4% of control values ($n = 3$, Fig. 2*E*).

Analysis of MA current kinetics revealed that the adaptation of RA currents was well fitted by two exponentials (Fig. 3*A*). Of the two derived time constants, $\tau 1$ was 2.93 ± 0.07 ms ($n = 126$) and described the initial very rapidly adapting component of the current, while $\tau 2$ was significantly longer, 53.05 ± 2.10 ms ($n = 126$) and described the later more slowly adapting part of the current. The amplitude of the component defined by $\tau 1$ accounted for most of the current (77.6 ± 1.3%) whereas the more slowly declining component accounted for 22.2 ± 0.7%. Peak MA current amplitude for a 16 μm stimulus for each narrow action potential (AP) neurone was compared to the size of $\tau 1$ and $\tau 2$ to determine if the kinetics of the current changed as the amplitude increased. Current amplitude had a small positive correlation with $\tau 1$ (Pearson's product moment; $r = 0.40$, $P < 0.01$; Fig. 3*B*) and a much stronger correlation with $\tau 2$ ($r = 0.88$, $P < 0.001$; Fig. 3*C*), i.e. current adaptation slowed with increasing current amplitude.

The kinetics of MA currents expressed by wide action potential neurones showed considerably more variation in their adaptation kinetics than did RA currents. Most MA currents were well fitted by a single exponential (example shown in Fig. 2*C*) whilst some were well fitted by two exponentials with a short $\tau 1$ that accounted for only a minor fraction of the current amplitude (i.e. < 20%). Such cells were pooled in the category of intermediately adapting (IA) currents. One wide AP cell responded with a slowly adapting (SA) MA current; such currents declined very little in amplitude over 200 ms and were also characterized by current amplitude reaching a peak during the stationary part of the stimulus (see for example Fig. 6*E*). This contrasts with both RA and IA currents where peak current amplitude occurred concurrently with cessation of probe movement.

Mechanically activated currents were unchanged in large DRG neurones derived from ASIC2 and/or ASIC3 null mutants

Price *et al.* (2000) have shown that Aβ-fibres from ASIC2 null mutants had decreased firing rates in response to mechanical stimuli. We therefore compared the MA currents of large neurones with narrow action potentials derived from ASIC2 KOs to wild-type controls. As can be seen in Fig. 4*A* the mechanosensitivity of neurones from these two genotypes was not significantly different (2-way, repeated-measures ANOVA; $P = 0.82$). The mean maximal amplitudes of MA currents were 2.66 ± 0.51 nA for KOs ($n = 21$) and 2.15 ± 0.55 nA for wild-types ($n = 21$). Similarly

the kinetics of MA currents were unaltered by the deletion of the ASIC2 gene (Fig. 4*B* and *D*); ASIC2 KO *versus* wild-type; $\tau 1 = 3.00 \pm 0.10$ ($n = 63$) *versus* 2.89 ± 0.08 ms ($n = 56$), $\tau 2 = 62.03 \pm 4.77$ ($n = 63$) *versus* 57.36 ± 4.17 ms ($n = 56$). All neurones with narrow APs from the ASIC2 KOs and 21/22 from wild-type controls were mechanosensitive and generated RA currents (Fig. 4*C*).

Despite strong evidence that ASIC2 subunits coassemble into heteromeric ASIC channels that mediate transient

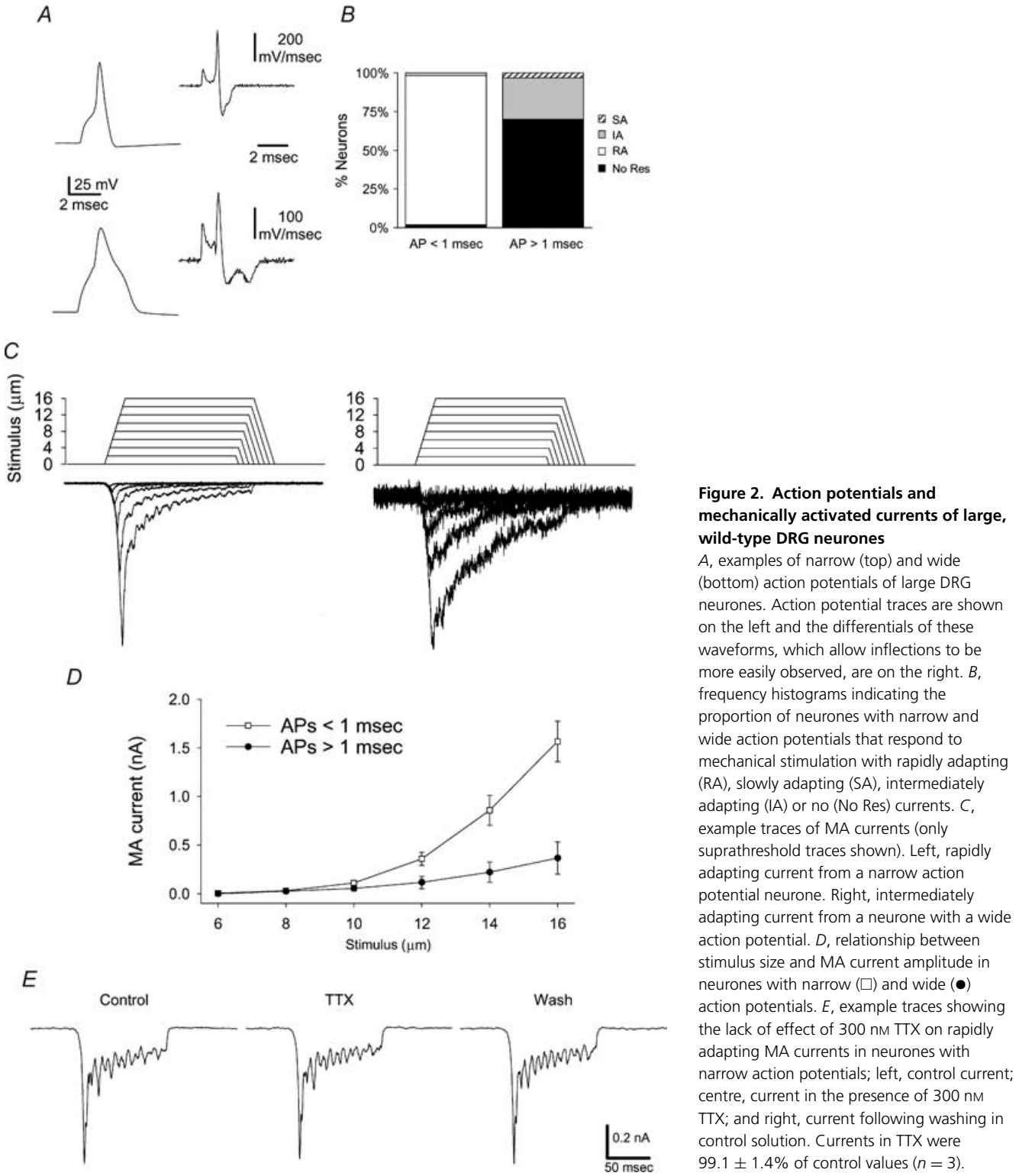

Figure 2. Action potentials and mechanically activated currents of large, wild-type DRG neurones
A, examples of narrow (top) and wide (bottom) action potentials of large DRG neurones. Action potential traces are shown on the left and the differentials of these waveforms, which allow inflections to be more easily observed, are on the right. *B*, frequency histograms indicating the proportion of neurones with narrow and wide action potentials that respond to mechanical stimulation with rapidly adapting (RA), slowly adapting (SA), intermediately adapting (IA) or no (No Res) currents. *C*, example traces of MA currents (only suprathreshold traces shown). Left, rapidly adapting current from a narrow action potential neurone. Right, intermediately adapting current from a neurone with a wide action potential. *D*, relationship between stimulus size and MA current amplitude in neurones with narrow (□) and wide (●) action potentials. *E*, example traces showing the lack of effect of 300 nM TTX on rapidly adapting MA currents in neurones with narrow action potentials; left, control current; centre, current in the presence of 300 nM TTX; and right, current following washing in control solution. Currents in TTX were $99.1 \pm 1.4\%$ of control values ($n = 3$).

low-pH gated currents, such currents in ASIC2 KOs show almost indistinguishable kinetics and amplitudes from wild-type currents (Price *et al.* 2000; Benson *et al.* 2002). In contrast, proton-gated currents are significantly slowed by the removal of ASIC3 (Price *et al.* 2001; Benson *et al.* 2002; Xie *et al.* 2002) and there is some alteration of mechanically evoked firing in RA Aβ-mechanoreceptors from these mutants (Price *et al.* 2001). We confirmed the slowing of proton-gated currents in ASIC3 nulls (see below) and then assessed MA current characteristics. We found that there was no change in either current amplitude (Fig. 4*A*) or in the response kinetics (Fig. 4*B* and *D*). Of neurones with narrow APs derived from ASIC3 nulls, 88.9% (8/9) were mechanosensitive and all had RA currents (Fig. 4*C*). The mean evoked current of responding neurones by a 16 μm stimulus was 1.45 ± 0.46 nA ($n = 8$) for ASIC3 nulls and 1.51 ± 0.74 nA ($n = 8$) for wild-types. Neither $\tau 1$ nor $\tau 2$ differed significantly: ASIC3 KO *versus* wild-type; $\tau 1 = 3.51 \pm 0.25$ ($n = 20$) *versus* 3.02 ± 0.18 ms ($n = 15$), $\tau 2 = 52.71 \pm 3.48$ ($n = 20$) *versus* 47.06 ± 5.55 ms ($n = 15$).

It has been suggested that there may be a significant amount of functional redundancy amongst the ASIC ion channel family or that in nulls there is functional compensation by related channels (Welsh *et al.* 2002). We therefore subsequently focused on the properties of MA currents of double KO (DKO) mice lacking the genes for both ASIC2 and ASIC3. There are currently no published investigations of such animals using the skin–nerve preparation but ASIC2 and ASIC3 are believed to heteromultimerize in DRG neurones (Benson *et al.* 2002) and are proposed to function cooperatively in mechanosensation (Welsh *et al.* 2002). Comparison of MA currents from large neurones with narrow APs showed that there was a trend towards currents being of smaller amplitude in the ASIC2/3 DKOs but this difference was not significant (Fig. 4*A* and 2-way, repeated-measures ANOVA; $P = 0.09$). Peak MA current amplitude in wild-types was 1.43 ± 0.28 nA ($n = 25$) compared to 0.93 ± 0.21 nA ($n = 25$) in DKOs. The removal of these two genes together did not alter the kinetics of the observed MA currents (Fig. 4*B* and *D*). ASIC2/3 DKO *versus* wild-type: $\tau 1 = 2.94 \pm 0.10$ ($n = 44$) *versus* 2.94 ± 0.13 ms ($n = 55$), $\tau 2 = 45.37 \pm 2.11$ ($n = 44$) *versus* 50.95 ± 2.09 ms ($n = 55$).

In all three KO strains large neurones with wide APs were either unresponsive to mechanical stimuli up to 16 μm (ASIC2 44.4% (8/18); ASIC3 100.0% (8/8); ASIC2/3 83.3% (5/6)) or displayed MA currents with IA kinetics, except for one ASIC2 KO neurone which had RA MA currents (AP width: 1.1 ms). In no mouse strain was the proportion of cells that did not respond different to that in wild-type controls (Fig. 4*C*). Also the mean amplitude of evoked responses did not differ between each KO strain and control (data not shown).

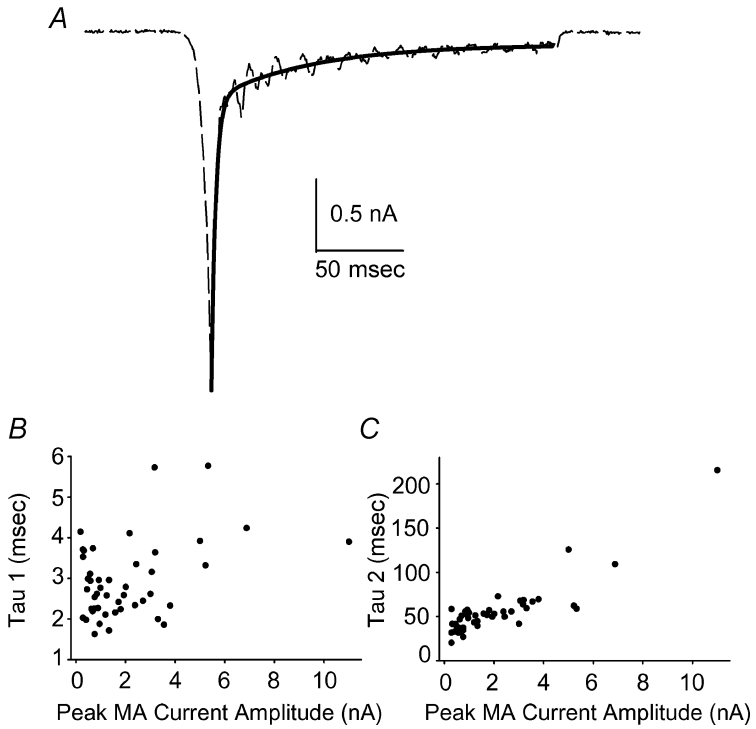

Figure 3. Decay of rapidly adapting MA currents is well described by two exponentials
A, example of the fitting of two exponentials (continuous line) to the decay of a MA current (dashed line). *B* and *C*, graphs show the relationship between peak current amplitude and the duration of $\tau 1$ (*B*) and $\tau 2$ (*C*) for RA MA currents evoked by a 16 μm stimulus ($n = 46$). In both cases there is a significant positive correlation between each variable for $\tau 1$, $r = 0.40$ (Pearson's product moment, $P < 0.01$) and for $\tau 2$, $r = 0.88$ ($P < 0.001$).

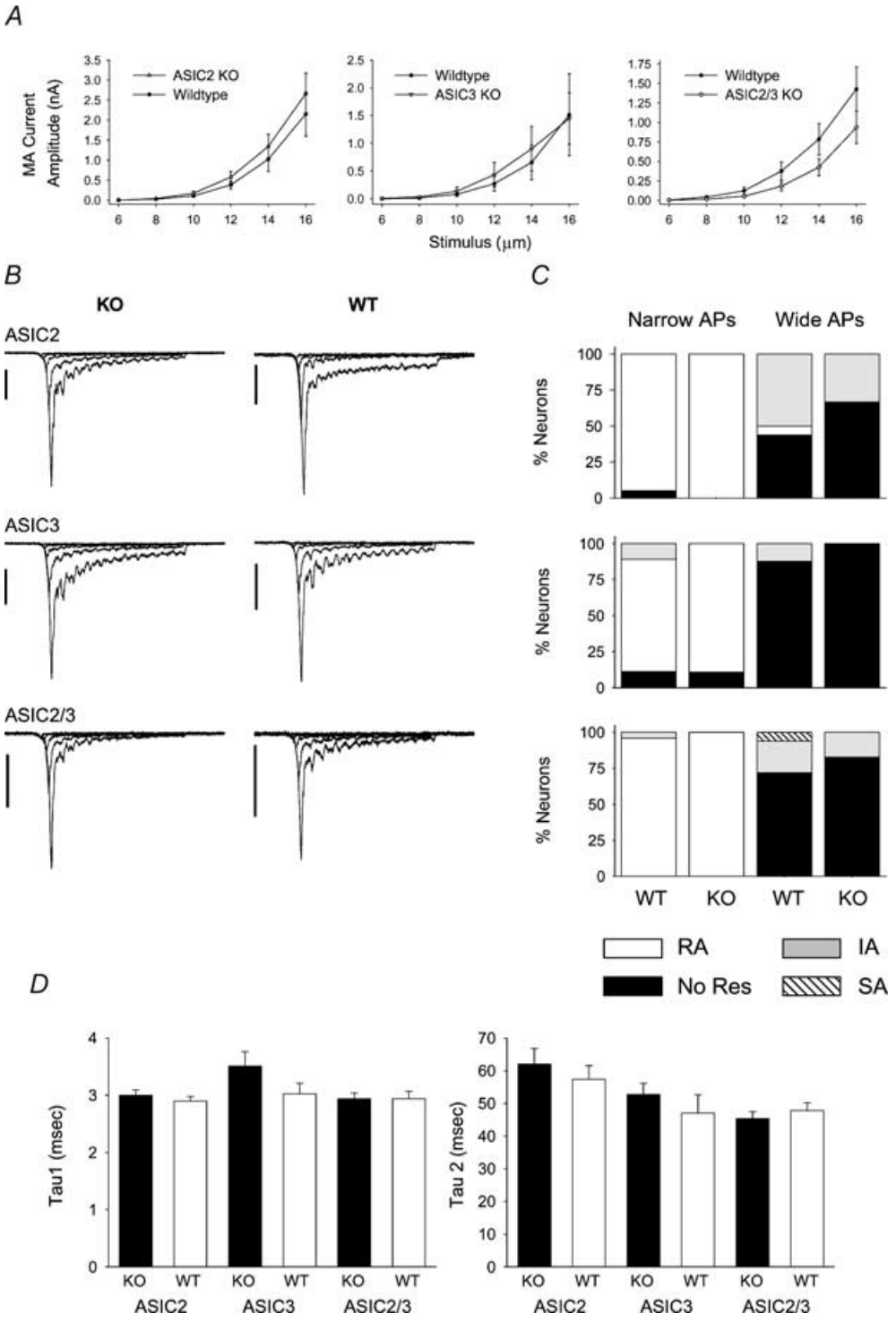

Figure 4. Comparison of MA currents in large neurones from wild-type and ASIC2 and/or 3 null mutants
A, graphs showing stimulus–response relationships for ASIC2 ($n = 21$), 3 ($n = 8$) and 2/3 ($n = 25$) knockouts (KO) *versus* wild-type controls ($n = 21$, 8 and 25, respectively). *B*, example traces of RA MA currents from narrow action potential neurones (scale bar is 1 nA in each trace). Left, traces from null mutants and, right, from wild-types for ASIC2 (top), ASIC3 (middle) and ASIC2/3 (bottom). *C*, frequency histograms for responses to mechanical stimulation of narrow (left) and wide (right) action potential neurones for null mutants (right) and wild-type controls (left). *D*, comparison of $\tau 1$ (left) and $\tau 2$ (right) values for RA MA currents between wild-type controls (open columns) and null mutants (filled columns): ASIC 2 (left), ASIC3 (centre) and ASIC2/3 (right).

Comparison of neuronal resting potential, AP duration, AP amplitude and AP dV/dt_{max} between genotypes for each strain revealed only one difference (see Table A, available online as Supplementary Material); dV/dt_{max} was significantly smaller in ASIC2/3 DKO narrow AP neurones *versus* wild-type; 368.00 ± 12.66 *versus* 432.20 ± 24.21 mV ms^{-1} (Student's unpaired *t* test, $P = 0.02$). The significance of this is unclear.

Ruthenium red voltage-dependently blocks mechanically activated currents

Previously we showed that ruthenium red blocked all MA currents in neonatal rat neurones with an IC_{50} value of around 4 μM (Drew *et al.* 2002). Here we tested the ability of 5 μM ruthenium red to inhibit MA currents in neurones that displayed RA inward currents from wild-type and ASIC2/3 DKOs. At a holding potential of −70 mV this concentration reduced responses by $43.27 \pm 4.57\%$ ($n = 5$) and $47.08 \pm 2.15\%$ ($n = 4$), respectively (Fig. 5*A* and *B*), indicating that there was no difference in phenotypes. Interestingly, it was observed that ruthenium red block of MA currents was strongly voltage dependent. MA currents are non-selective cation currents with a reversal potential of around 0 mV in quasi-physiological solutions (L. J. Drew & P. Cesare, unpublished data). When 5 μM ruthenium red was applied to neurones held at +70 mV, outward MA currents were not inhibited in either genotype (ASIC2/3 DKO: $97.53 \pm 4.53\%$, $n = 3$, of control *versus* wild-type: $95.02 \pm 7.52\%$, $n = 2$) (Fig. 5*A* and *C*).

Mechanically activated currents in small–medium neurones from wild-type and ASIC2/3 null mutants

Responses of small–medium diameter (< 35 μm, mean 29.52 ± 0.38 μm) DRG neurones to mechanical stimulation were also tested and wild-type responses were compared to those of ASIC2/3 DKOs. Nearly all small–medium neurones exhibited wide action potentials (88.2%, 45/51) and overall 51.0% (26/51) of them responded to mechanical stimulation up to 12 μm. We subdivided neurones firstly according to whether they bound the isolectin IB4.

The mechanical response properties of neurones that did not bind IB4 (IB4–) fell into four categories: 51.4%

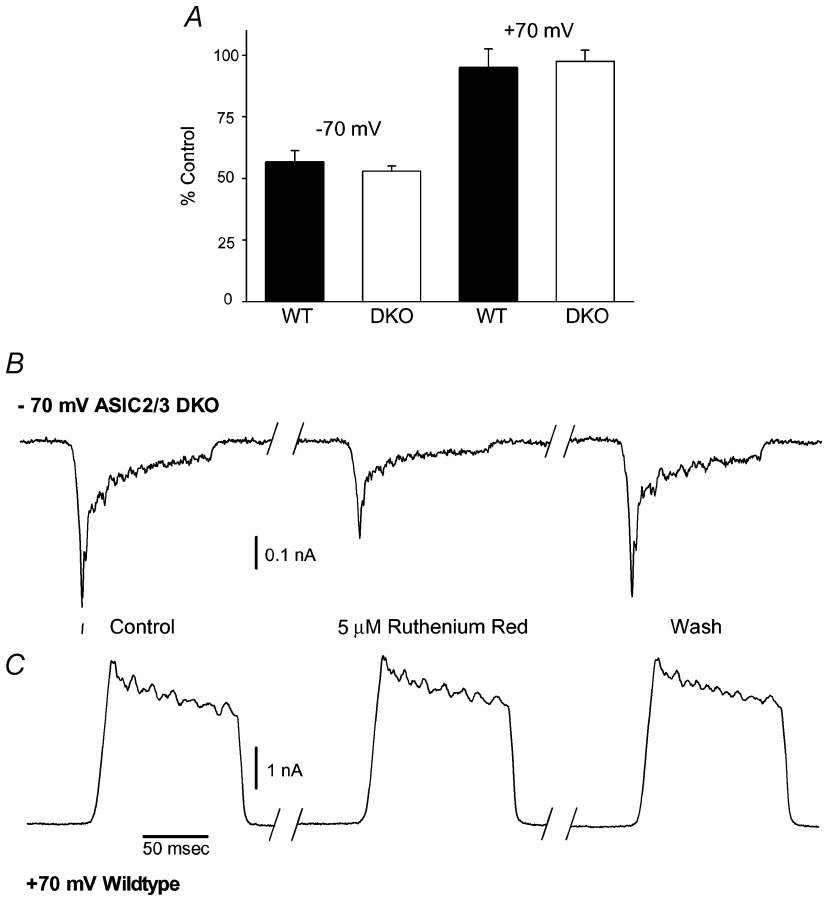

Figure 5. RA MA currents are voltage dependently blocked by ruthenium red
A, inhibition of RA MA currents by 5 μM ruthenium red at a holding potential of −70 mV (left) and +70 mV (right) in wild-type (filled columns) and ASIC2/3 double knockouts (DKOs) (open columns). *B*, example traces of ruthenium red blockade of MA currents in a wild-type neurone held at −70 mV. *C*, example traces showing no effect of ruthenium red at +70 mV in an ASIC2/3 DKO neurone.

(18/35) of wild-type neurones did not respond to stimulation up to 12 μm, 17.1% (6/35) responded with RA currents, 14.3% (5/35) had IA currents and 17.1% (6/35) displayed SA currents (Fig. 6*A* and *C–E*). The kinetics of RA currents and IA currents were similar to those observed in large neurones. RA currents (Fig. 6*C*) were well fitted by two exponentials, $\tau 1$ (2.64 ± 0.21 ms, $n = 8$) described the initial very rapidly adapting component, and the longer $\tau 2$ (48.90 ± 6.39 ms, $n = 8$) described the second slowly decaying part of the response. IA currents (Fig. 6*D*) were again a mixture of those well described by a single exponential and those better described by two, but with the fast τ accounting for a minor part of the current. SA currents (Fig. 6*E*) were more prevalent amongst small nociceptive neurones than amongst large neurones.

MA currents observed in small IB4– neurones derived from ASIC2/3 DKO showed no significant differences from those seen in wild-type neurones. The proportion of neurones attributed to each category was not altered: 52.0% (13/25) did not respond, 12.0% (3/25) showed RA currents, 24.0% (6/25) had IA currents and 12.0% (3/25) had MA currents that adapted slowly (χ^2; $P = 0.73$,

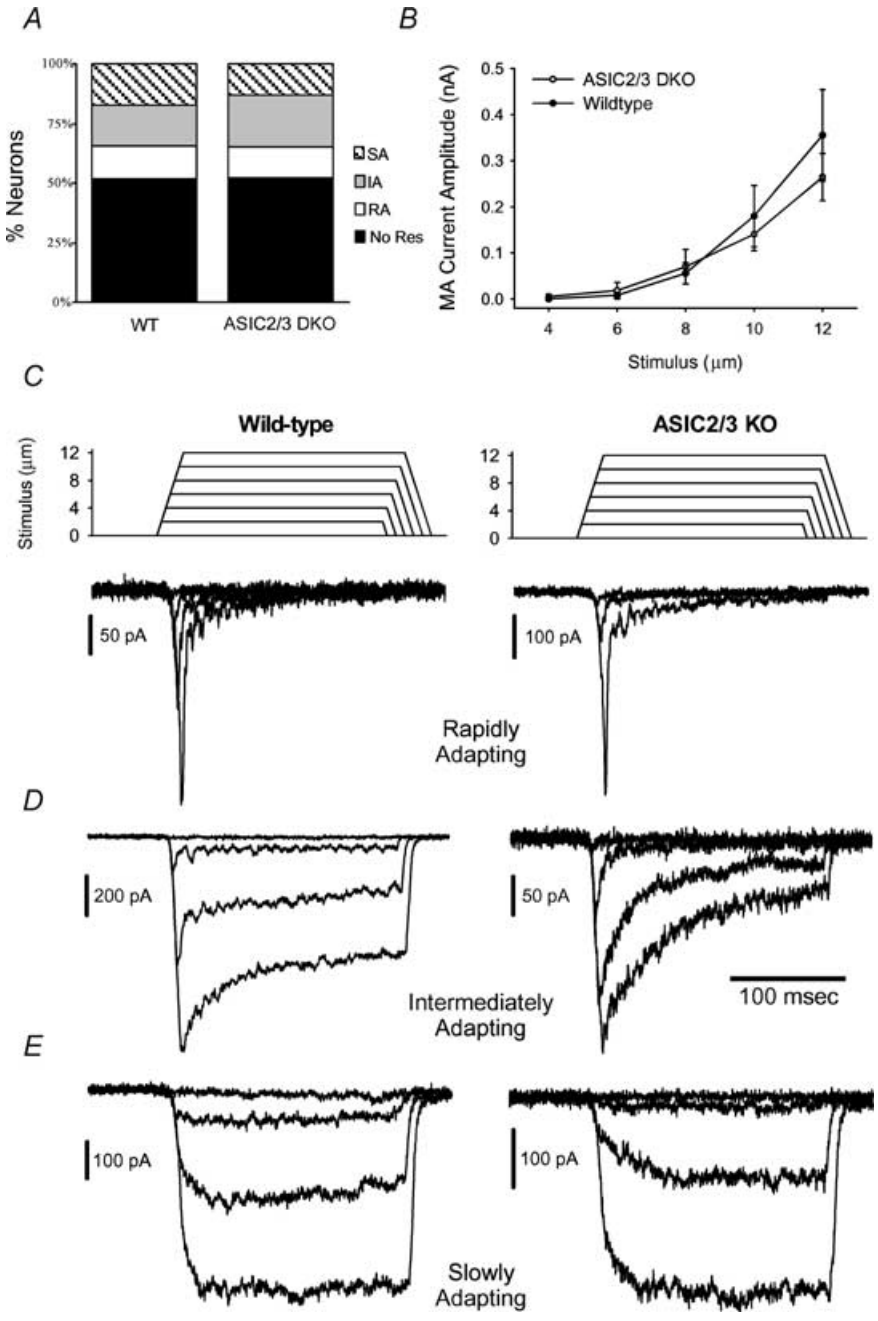

Figure 6. MA currents exhibited by wild-type and ASIC2/3 DKO IB4– small–medium DRG neurones
A, frequency histograms for responses of wild-type and ASIC2/3 DKO neurones; responses were of four types – slowly (SA), rapidly (RA) or intermediately (IA) adapting currents, or no response (No Res). *B*, comparison of stimulus–response relationships for pooled data from IA and SA currents of wild-type (●, $n = 11$) and ASIC2/3 DKO (○, $n = 9$) neurones. *C–E*, example traces of RA, IA and SA currents, respectively, from wild-type (left) and ASIC2/3 DKO (right) neurones.

Table 1. Response properties of IB4-negative small–medium neurones defined by their response to mechanical stimulation

MA current	Genotype	AP > 1 ms	TTX-r	Capsaicin	pH 5.3	T:S:M
RA	WT	1/6	1/5	0/5	5/5	4 : 1 : 0
	DKO	1/3	2/3	0/3	2/2	1 : 1 : 0
SA	WT	6/6	5/5	1/5	5/5	3 : 1 : 1
	DKO	3/3	2/2	0/2	1/2	0 : 1 : 0
IA	WT	5/5	5/5	2/5	5/5	4 : 1 : 0
	DKO	5/5	5/5	2/4	4/4	2 : 2 : 0
No response	WT	17/18	15/16	8/16	16/16	8 : 5 : 3
	DKO	11/12	12/12	5/11	10/10	6 : 4 : 0

The table shows the fraction of neurones in each category (RA, rapidly adapting; SA, slowly adapting; IA, intermediately adapting) that have action potential (AP) durations over 1 ms, respond to capsaicin, express TTX-r sodium currents and respond to pH 5.3. The final column indicates the kinetics of responses to pH 5.3: T, transient current; S, slow (persistent currents/TRPV1-mediated responses); M, mixed currents. WT, wild-type; DKO, double knockout mice.

Fig. 6*A*). Similarly, within each group the kinetics of the responses were not altered by the gene deletions (Fig. 6*C–E*). For RA currents $\tau 1$ was 2.92 ± 0.37 ms ($n = 6$) and $\tau 2$ was 49.81 ± 8.04 ms ($n = 6$). The mean evoked current amplitude of this class of neurones was unaltered in the DKOs. The stimulus–response curves for pooled IA and SA MA currents are shown in Fig. 6*B* (2-way ANOVA, repeated measures; $P = 0.37$). No differences were seen between RA, SA and IA groups when analysed separately (data not shown).

Examination of the physiological properties of neurones classified according to their responses to mechanical stimulation revealed some trends within groups (see Table 1). The majority of neurones that expressed RA currents also fired narrow APs (4/5 in wild-types and 2/3 in DKOs) and none responded to capsaicin. Neurones with SA currents were largely capsaicin insensitive (wild-type: 5/6, DKO: 2/2) but all expressed wide APs. Nearly all unresponsive neurones (wild-type: 17/18, DKO: 11/12) and IA MA current neurones (wild-type: 6/6, DKO: 4/4) had wide APs. Within these groups, in both genotypes, approximately half of the cells responded to capsaicin (see Table 1).

Interestingly, action potentials of IB4– nociceptors were significantly longer in DKO neurones than in wild-type neurones (2.87 ± 0.33 ms ($n = 22$) *versus* 1.92 ± 0.13 ms ($n = 29$), Student's unpaired *t* test, $P = 0.01$), which may in part be related to a lower maximal rate of change of membrane potential in DKO neurones (230.48 ± 17.36 mV ms^{-1} *versus* 272.41 ± 12.32 mV ms^{-1}, $P < 0.05$).

In IB4-binding (IB4+) neurones it was found that both wild-type and ASIC2/3 DKO neurones were either unresponsive to mechanical stimulation or responded with IA currents. In each case the proportion was approximately 50%; in wild-type neurones 56.3% (9/16) responded whilst in DKOs 50.0% (10/20) responded (Fig. 7*A*). The mechanosensitivity of responding neurones was not significantly different between genotypes (2-way ANOVA, repeated measures; $P = 0.70$, Fig. 7*B*). Mean maximal currents were 434.05 ± 76.45 pA in DKOs and 360.88 ± 105.70 pA in wild-types. Residual currents were observed in these neurones that persisted after the withdrawal of the mechanical stimulus (e.g. Fig. 7*C*). Such currents were not observed in other cell types and their significance is unclear. There were no differences in the physiological parameters of IB4+ neurones between genotypes or between those that responded to mechanical stimulation and those that did not (see Table A in online Supplementary Material).

In neonatal rat, IB4+ neurones were essentially refractory to mechanical stimulation (Drew *et al.* 2002) suggesting that there is either a species or a developmental difference that accounts for the observation of MA currents in the adult mouse IB4+ cells. To distinguish between these possibilities IB4+ neurones from young adult (p28) rats were mechanically stimulated. In 16 neurones tested 43.8% (7/16) exhibited MA currents and of these 85.7% (6/7) displayed IA currents whilst the other cell had SA kinetics (see Fig. 7*A* and *C*). The mean maximal evoked current was 0.30 ± 0.08 nA.

Comparison of wild-type IB4+ and IB4– nociceptors (i.e. neurones selected for having wide, inflected APs) revealed a number of differences between these two groups of cells. As previously reported by Stucky & Lewin (1999) IB4+ neurones had significantly longer action

potentials than IB4– neurones (2.85 ± 0.17 ms *versus* 1.92 ± 0.13 ms, Student's unpaired t test, $P < 0.001$). However, in our recording configuration a number of other differences were apparent; most notably, the resting membrane potential of IB4+ neurones was more depolarized than that of IB4– neurones (-51.92 ± 0.87 mV *versus* -58.03 ± 0.76 mV, Student's unpaired t test $P < 0.001$). Action potentials (recorded at a potential of -70 mV) were also significantly larger in IB4+ cells (145.59 ± 0.83 mV *versus* 139.29 ± 1.09 mV, $P < 0.001$) and the maximal rate of change of membrane potential was higher in IB4– neurones (272.41 ± 12.32 mV ms^{-1} *versus* 232.19 ± 8.10 mV ms^{-1}, $P < 0.05$) (see Table A in online Supplementary Material).

Low pH and capsaicin-evoked currents in wild-type and ASIC2/3 null DRG neurones

As well as studying the association between ASICs and mechanosensitivity, we also categorized the responses of different classes of DRG neurone to low pH (pH 5.3) and investigated the previously unreported response properties of neurones lacking the genes for ASIC2 and 3. As before, neurones were classified according to size, action potential duration and IB4 binding. Responses to low pH fell into three classes: transient ASIC-like responses, slowly activating, persistent currents or mixed currents (in which a small transient current was activated prior to a slowly activating, persistent component) (see Figs 8*B* and 9*B*).

Application of pH 5.3 solution to wild-type, large neurones evoked an inward current in 90.7% (49/54) of cells; the proportion of positive responses was similar amongst wide (85.7%; 18/21) and narrow (93.9%; 31/33) action potential classifications. However, the division of responses according to desensitization kinetics revealed significant differences between the two neuronal classes. Amongst neurones with narrow action potentials the predominant response was a slowly activating, persistent current seen in 71.0% (22/31) of responding neurones (Fig. 8*A* and *B*). In contrast, no neurones with a

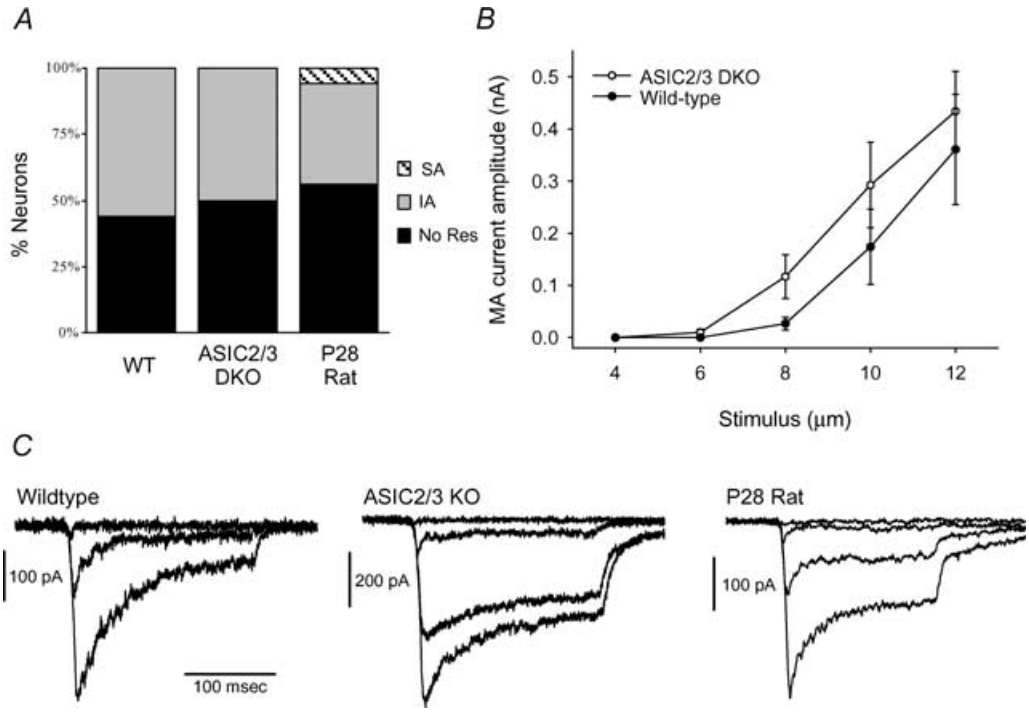

Figure 7. MA currents exhibited by adult rat, wild-type mouse and ASIC2/3 DKO mouse IB4+ DRG neurones

A, frequency histogram showing that approximately half of IB4+ neurones from wild-type (56.3%, left) and ASIC2/3 DKO (50.0%, centre) mice exhibited intermediately adapting MA currents whilst the remainder were unresponsive to mechanical stimulation. In the adult rat 56.3% of neurones did not respond; of those that did 6/7 had intermediately adapting kinetics and the seventh was slowly adapting. *B*, comparison of stimulus–response relationships for wild-type (●, $n = 9$) and ASIC2/3 DKO (○, $n = 10$) neurones from mice showing no significant difference between these populations. *C*, examples of MA current traces from a wild-type (left) and an ASIC2/3 DKO (centre) mouse neurone and an adult rat neurone (right).

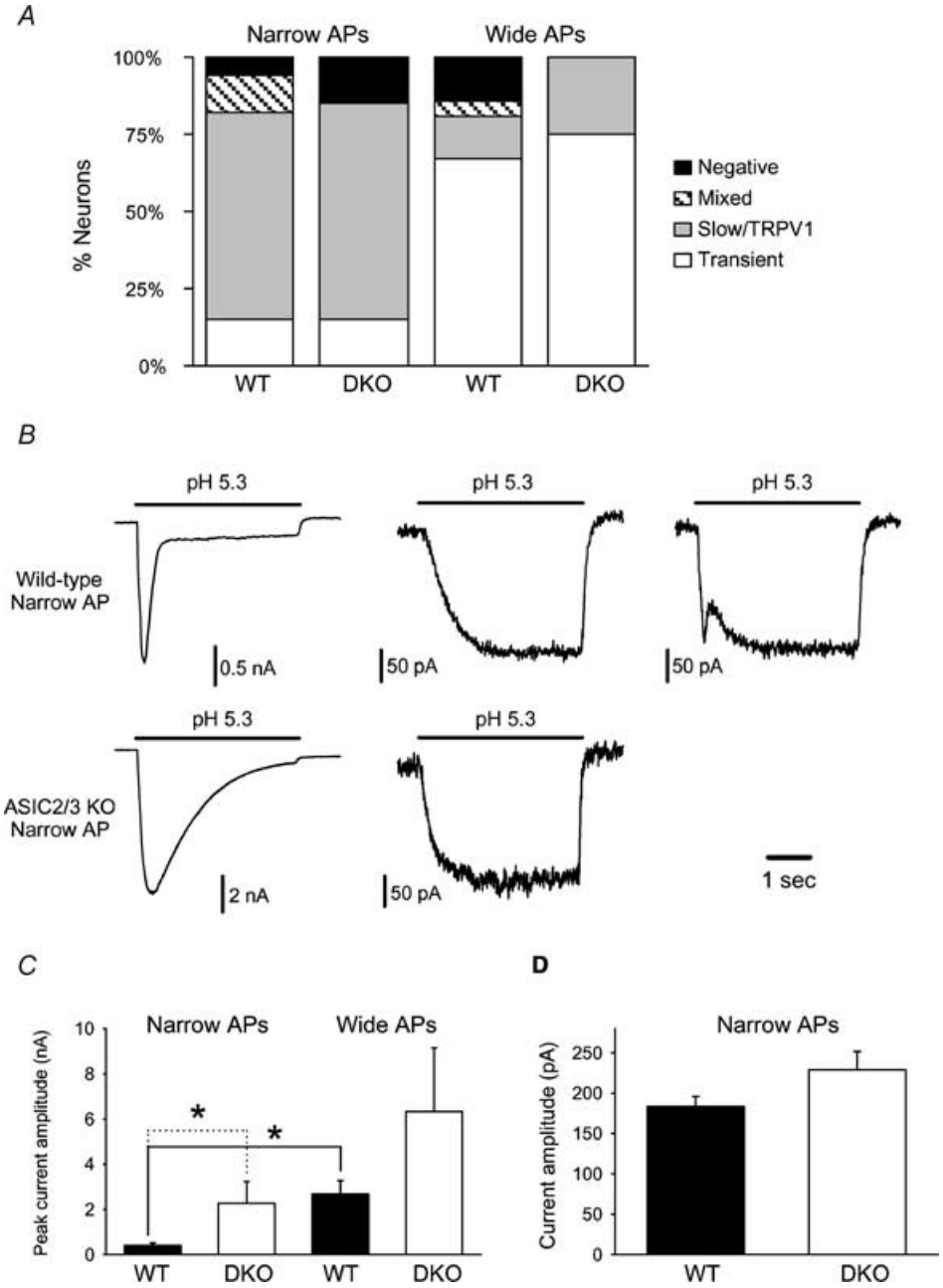

Figure 8. Currents activated in large DRG neurones by pH 5.3; comparison of ASIC2/3 DKO and wild-type neurones

A, frequency histograms of the responses of different neuronal populations to pH 5.3. Left, large neurones with narrow action potentials; right, large neurones with wide action potentials; wild-type columns are on the left and nulls on the right. Responses were classified as Transient, Slow/TRPV1 (slowly activating persistent currents or currents probably mediated by TRPV1), Mixed (initial transient peak followed by slowly activating persistent current) or Negative (non-responsive). Mixed currents were absent from ASIC2/3 DKO neurones, otherwise the proportions of each type of response were similar in each subpopulation. *B*, example traces from wild-type (top) and ASIC2/3 DKO (bottom) large, narrow action potential neurones. *C*, mean peak current amplitudes of transient proton-gated currents. Currents generated by large neurones with narrow action potentials (left) and wide action potentials (right); wild-type (filled columns) and ASIC2/3 DKO (open columns). In wild-types, responses of wide action potential cells were significantly larger than those of narrow action potential cells ($P < 0.05$). ASIC2/3 DKOs had larger currents than wild-types in narrow action potential neurones ($P < 0.05$) and there was a similar trend between wide action potential neurones ($P = 0.054$). *D*, mean current amplitudes of persistent proton-gated currents in large neurones with narrow action potentials; wild-type (filled column) and ASIC2/3 DKO (open column).

wide action potential showed such a response in the absence of a transient component. Instead, amongst this population 77.8% (14/18) neurones expressed transient currents typical of those mediated by ASICs (Fig. 8*A* and *B*). Transient proton-gated currents were seen in only 16.1% (5/31) of narrow action potential neurones. Moreover, the amplitudes of transient currents were significantly larger in neurones with wide action potentials, 2.67 ± 0.60 nA, than in narrow action potential neurones, 0.39 ± 0.12 nA (t test, $P < 0.05$, Fig. 8*C*). In both groups the duration and profile of the transient component was similar (τ desensitization, narrow action potential: 126.8 ± 16.6 ms, wide action potential: 194.2 ± 26.4 ms, $P = 0.12$), whereas the fractional amplitude of the sustained component varied. The amplitude of persistent currents was consistently small, the mean maximal amplitude amongst wild-type neurones with narrow action potentials was 197.4 ± 18.6 pA ($n = 22$, Fig. 8*D*). This also suggests that larger transient proton-gated currents may have masked such currents in some neurones. 'Mixed' currents were seen in 12.9% (4/31) of narrow action potential neurones and 5.6% (1/18) of wide action potential cells (Fig. 8*A* and *B*). In three capsaicin-sensitive wide action potential neurones the response kinetics indicated that the currents were likely to be mediated solely by TRPV1 (data not shown). Consistent with our previous observations (Drew *et al.* 2002) there was no correlation between the amplitude or type of response to low pH and the response to mechanical stimulation.

In large ASIC2/3 DKO neurones the proportions of neurones with slow and transient currents were similar to wild-type although mixed currents were not observed. Amongst narrow action potential cells, 85.0% (17/20) responded to protons; 82.4% (14/17) had persistent currents and 17.6% (3/17) had transient responses (Fig. 8*A* and *B*). Four of four neurones with wide action potentials responded; 3/4 had transient currents and the remaining neurone displayed a slowly activating persistent current. The desensitization kinetics of transient currents were similar in both groups and were much slower in DKO neurones than in wild-type neurones (Fig. 8*B*). The τ of desensitization was 1.06 ± 0.08 s for narrow action potential neurones and 1.15 ± 0.02 s in wide action potential cells. There was a tendency for transient currents to be of larger amplitude in DKO neurones; in neurones with narrow action potentials the mean amplitude was 2.28 ± 0.96 nA ($n = 3$, $P = 0.04$ *versus* wild-type, Fig. 8*C*) and in wide action potential neurones it was 6.33 ± 2.82 ($n = 3$, $P = 0.054$ *versus* wild-type, Fig. 8*C*). Slowly activating persistent currents were slightly larger in DKO neurones but the difference was not significant; the mean amplitude was 229.4 ± 21.2 pA ($P = 0.07$ *versus* wild-type, Fig. 8*D*). Changes in transient low pH-evoked current kinetics in ASIC2 and ASIC3 knockouts were consistent with the effects published by Benson *et al.* (2002) and Xie *et al.* (2002) (data not shown). However, while mixed kinetic currents were present in ASIC2 knockout neurones, they were absent from ASIC3 knockouts.

Only 4.3% (2/46) of large wild-type neurones with narrow action potentials responded to capsaicin (both responses were small, < 250 pA, and one of these cells generated a TTX-r sodium current). However, 25.0% (8/32) of large, wide action potential neurones were capsaicin sensitive. These responses varied widely in amplitude but tended to be larger than those of narrow action potential cells; the mean evoked current was 4.05 ± 2.36 nA (data not shown).

We then examined pH 5.3-evoked currents in small–medium nociceptive neurones, i.e. those with wide action potentials. Nearly all IB4– nociceptors responded to a pH 5.3 stimulus (wild-type: 100.0% (26/26), and ASIC2/3 DKO: 93.3% (15/16)). Responses to pH 5.3 in relation to responses to mechanical stimulation are summarized in Table 1. Amongst wild-type neurones transient proton-gated currents were present in 50.0% (13/26) of cells, mixed currents in 15.3% (4/26) and persistent currents in 34.6% (9/26), three of which were probably TRPV1 mediated (Fig. 9*A* and *B*). In ASIC2/3 DKO neurones only sustained and transient currents were observed, transient in 46.7% (7/15) of responding neurones and sustained currents in 53.3% (8/15) (Fig. 9*A* and *C*), two of which were likely to be due to TRPV1 activation. Amongst either mutant or control nociceptors, the desensitizing components of transient currents were kinetically similar whereas the sustained components of these currents were more varied often due to the slow activation of TRPV1 receptors (data not shown, the example shown in Fig. 9*C* was capsaicin insensitive). Between genotypes the τ of desensitization of transient currents differed significantly; in wild-types it was 130.49 ± 6.56 ms ($n = 13$) compared to 1.41 ± 0.01 s ($n = 7$) in DKOs. Transient currents were also significantly larger in ASIC2/3 DKO neurones, 5.25 ± 0.93 nA *versus* 2.06 ± 0.58 nA (Student's unpaired t test, $P < 0.01$), due mainly to a large reduction in the number of cells that expressed small (< 0.5 nA) transient currents in the mutant genotype. The amplitude of persistent currents was similar in DKO (116.1 ± 25.8 pA) and wild-type (125.8 ± 37.9 pA, $P = 0.84$) neurones and mixed kinetics currents were consistently small (69.4 ± 5.2 pA).

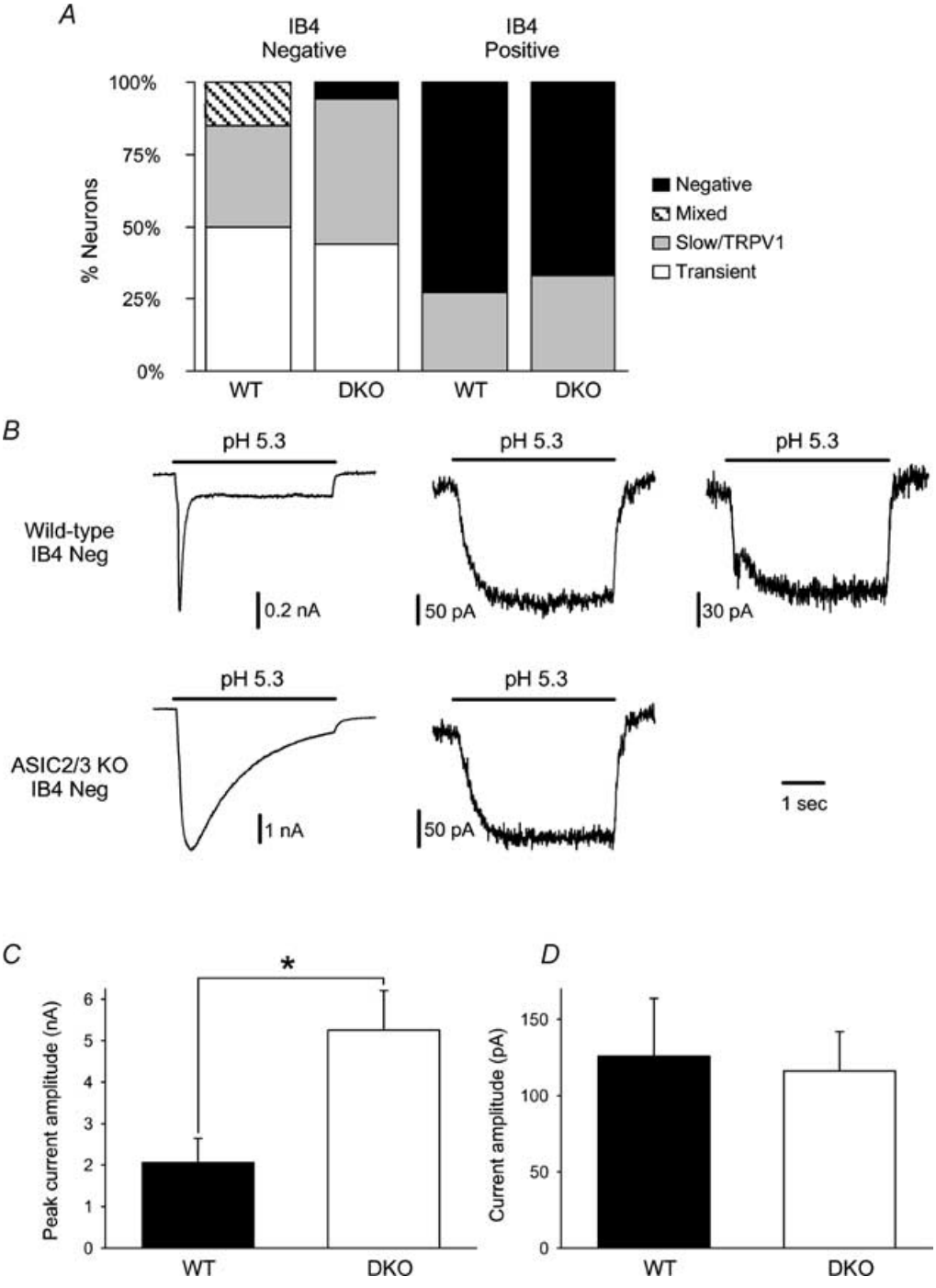

Figure 9. Currents activated in small–medium DRG neurones by pH 5.3; comparison of ASIC2/3 DKO and wild-type neurones

A, frequency histograms of the responses of different neuronal populations to pH 5.3. Left, IB4– nociceptors, and right, IB4+ nociceptors; wild-type columns are on the left and nulls on the right. Responses were classified as Transient, Slow/TRPV1, Mixed or Negative. In IB4– neurones the proportion of cells displaying transient currents was similar between genotypes (wild-type, 50.0%; DKO, 43.8%); mixed currents were absent from ASIC2/3 DKO neurones. The majority of IB4+ neurones did not respond to acidification and transient proton-gated currents were not observed in these cells. No distinction between genotypes was seen. *B*, example traces from wild-type (top) and ASIC2/3 DKO (bottom) IB4– neurones with wide action potentials. *C*, mean peak amplitude of transient currents in wild-type (filled column) and ASIC2/3 DKO (open column) IB4– nociceptors; currents were significantly smaller in wild-type neurones ($P < 0.01$). *D*, mean amplitude of persistent currents in capsaicin-insensitive wild-type (filled column) and ASIC2/3 DKO (open column) IB4– nociceptors. No difference was found between genotypes.

As observed by Dirajlal *et al.* (2003) transient acid-evoked currents were absent from IB4+ neurones (Fig. 9*A*). In wild-type neurones 26.7% (4/15) tested for proton sensitivity showed small (<100 pA) sustained responses and 26.7% (4/15) were sensitive to capsaicin, three neurones responded to both. In DKO neurones 40.0% (6/15) responded to low pH (5/6 currents < 100 pA and the sixth (248 pA) had kinetics characteristic of a TRPV1-mediated response) and 16.7% (3/18) responded to capsaicin, one cell was sensitive to both (data not shown).

Discussion

We have shown that clearly defined subsets of adult, sensory neurones have distinct responses to mechanical stimulation and that these responses are not mediated by ASIC2 or ASIC3. In this study we used cell size, action potential duration and IB4 binding to classify neurones. *In vivo* studies have shown a robust correlation between action potential duration and mechanical sensitivity; receptors with high mechanical thresholds and mechanically insensitive neurones express wide, inflected action potentials regardless of fibre type whereas narrow action potentials are displayed almost exclusively by Aβ- and Aδ-fibre low threshold mechanoreceptors (Rose *et al.* 1986; Koerber *et al.* 1988; Ritter & Mendell, 1992; see Lawson, 2002). Here we have also found a striking relationship between action potential duration and responses to mechanical stimulation *in vitro*. Nearly all large neurones expressing narrow action potentials displayed significant inward cationic currents that adapted rapidly. By comparison, similar sized neurones with wide, inflected action potentials responded much less frequently to mechanical stimulation (within the testing range) and overall had currents that were much smaller and displayed distinct rates of adaptation. The adaptation of rapidly adapting currents was well described by two exponentials indicating a rapidly adapting initial phase followed by a slowly adapting component, the slow phase tending to slow as current amplitude increased.

Small–medium neurones, the vast majority of which exhibited wide action potentials indicative of nociceptors, exhibited four categories of responses to mechanical stimulation. Approximately half were unresponsive when subjected to displacements (up to 12 μm) whilst the remainder had responses that were classified as rapidly, intermediately or slowly adapting. The predominant MA currents had intermediate adaptation kinetics; such responses were seen in IB4– neurones and were characteristic of all responding IB4+ neurones. Hence intermediately adapting currents appear to be the response of the majority of nociceptive neurones to membrane displacement. Subpopulations of IB4– neurones also displayed slowly and rapidly adapting currents. The identity of neurones that display slow responses is unclear although the observed distribution and frequency is consistent with them being Aδ-mechanonociceptors (Koltzenburg *et al.* 1997). The majority of small–medium neurones that exhibited MA currents with rapidly adapting kinetics also displayed narrow action potentials and it is possible that these smaller neurones are also low threshold mechanoreceptors (Djouhri *et al.* 1998; Lawson, 2002). Thus our data are consistent with investigations of mechanosensitivity in the intact animal.

To investigate the molecular basis of MA currents in DRG neurones we determined if neurones derived from ASIC2 and ASIC3 null mutants showed altered responses to focal mechanical stimulation. First we examined putative low threshold mechanoreceptor neurones. Price *et al.* (2000, 2001) observed that mechanically evoked firing in Aβ-fibres from ASIC2 nulls was reduced and that there was an increase in firing rates in RA-mechanoreceptors from ASIC3 knockout mice. Although our *in vitro* system prohibits direct comparison of the different subclasses of Aβ-fibres characterized by Price *et al.* (2000, 2001), the data demonstrate that the deletion of these genes, alone or together, had no significant effect on either the sensitivity of large neurones with narrow action potentials to mechanical stimulation or on the kinetics of evoked responses. We therefore conclude that neither of these ion channels contributes to the generation of MA currents in isolated neurones. Mechanically evoked responses of small–medium and other large neurones also showed no differences between wild-type and double knockout neurones. Price *et al.* (2001) showed a reduced sensitivity of Aδ-nociceptors in ASIC3 nulls but no subpopulation showed any decrease in sensitivity in our assay.

There was a notable (but not statistically significant) difference in the mean amplitude of MA currents between ASIC2 nulls and wild-type controls and ASIC3 nulls and controls. This may be due to the different genetic backgrounds of these mouse strains (see Methods) and variation introduced by crossing the two lines may account for the small difference between ASIC2/3 DKOs and controls.

The observations that around half of adult mouse and rat, but not neonatal rat (Drew *et al.* 2002), IB4-positive neurones generate MA currents suggest that developmental changes occur in the mechanosensitivity

of these neurones. One possibility is that neurotrophic signalling modulates mechanosensitivity as such signalling undergoes major postnatal changes in IB4-positive neurones (Molliver *et al.* 1997). Brain-derived neurotrophic fctor (BDNF) has been shown to regulate the mechanosensitivity of slowly adapting mechanoreceptors (Carroll *et al.* 1998) and in IB4-positive neurones Stucky *et al.* (2002) have shown that GFRα2 (glial cell-line derived neurotrophic factor family receptor) null mutants have a selective reduction in their sensitivity to heat stimuli. Alternatively, as IB4 binds a greater proportion of neurones in the adult than the neonate (Bennett *et al.* 1996) it may be the case that with development IB4 comes to label a population of mechanically sensitive neurones.

Our investigation of responses to low pH revealed that distinct current types are differentially distributed amongst the categories of DRG neurones we defined. The major currents observed in response to extracellular acidification were ASIC-mediated transient currents and a slowly activating persistent current, although a small number of cells displayed both types of currents. Our data suggest that functional expression of ASIC-like currents is found predominately in IB4-negative neurones likely to have a nociceptive function. Amongst large neurones approximately 75% of those with wide action potentials (almost certainly IB4-negative due to the size distribution of IB4-binding neurones: Molliver *et al.* 1997; Dirajlal *et al.* 2003) displayed transient proton-gated currents whereas in those with narrow action potentials the expression frequency was below 20%. In small–medium neurones, approximately 50% of IB4-negative nociceptors exhibited transient proton-gated currents whereas, in agreement with Dirajlal *et al.* (2003), we did not observe such currents in IB4-positive cells. Two aspects of our data support the hypothesis that ASIC1, 2 and 3 subunits are usually coexpressed and form heteromeric ion channels (Benson *et al.* 2001; Xie *et al.* 2002): Firstly, in wild-type neurones the rate of desensitization of all transient currents was rapid and consistent with the coexpression of all three subunits (Benson *et al.* 2001) whereas in the double knockout transient currents all displayed desensitization kinetics consistent with the expression of ASIC1 (Waldmann *et al.* 1997; Chen *et al.* 1998) (although it is unclear if ASIC1a or 1b or a combination of the two mediated the responses we observed). Secondly, transient currents were seen in similar proportions of neurones derived from wild-type and ASIC2/3 double knockouts. However, it was notable that neurones lacking ASIC3 did not generate mixed currents suggesting ASIC3 is sometimes expressed without other ASIC subunits. The tendency for pH 5.3-evoked currents to be larger in ASIC2/3 double knockouts may reflect an up-regulation of ASIC1 transcripts, although the slowed rate of desensitization would be likely to contribute to the increase in peak current.

The other major response to acidification that we observed was a slowly activating, persistent current. Interestingly, this was the most common response of presumptive low threshold mechanoreceptors to pH 5.3 (seen in around 70–80% of neurones) but was also seen in all other neuronal subtypes. Persistent currents have been reported before in capsaicin-insensitive cells (Petruska *et al.* 2000) but have not been functionally characterized. The channel that underlies this response is unknown; such currents were present in ASIC2/3 double knockouts and also in ASIC1 nulls and were insensitive to 200 μM amiloride (L. J. Drew & D. K. Rohrer, unpublished observations). The slow kinetics of current activation were similar to those observed for TRPV1 gating; however, this current was observed mainly in capsaicin-insensitive neurones. We found such currents most frequently in large neurones with narrow action potentials (although they may have been present, but masked, in neurones with large ASIC-mediated currents). The absence of large transient proton-gated currents in the majority of presumptive low threshold mechanoreceptors is consistent with the acid insensitivity of their peripheral endings (Lewin & Stucky, 2000), although the activation of a persistent inward current by low pH could have important consequences for neuronal excitability.

Most research in the mechanosensation field suggests that transduction is a process intrinsic to sensory neurones (Lewin & Stucky, 2000). Hence, the finding that separate classes of neurones display characteristic MA currents consistent with their predicted function *in vivo*, strongly suggests that the type of mechanosensitive ion channels found at the soma are important in mechanosensation. We propose that these channels are normally present at sensory endings and contribute to the transduction of mechanical force into action potentials. The diversity in MA current kinetics and other characteristics may be accounted for by the expression of distinct but closely related ion channels or by different heteromeric compositions of channels. Alternatively, the behaviour of the same channel may be influenced by interactions with different membrane proteins or lipids or different cytoskeletal elements. These hypotheses are supported, but not distinguished, by the findings that different neuronal subpopulations show similar degrees of inhibition by ruthenium red and gadolinium but are differentially affected by cytochalasin B and changes in external [Ca^{2+}] (Drew *et al.* 2002). In culture, these channels can generate considerable whole-cell currents in the absence of a

complex extracellular matrix, although this does not preclude their modulation by extracellular binding proteins. It may be the case that interacting proteins alter the sensitivity of the channel or its kinetics.

The identity of the ion channels underlying the observed MA currents remains unknown. Amongst candidate receptor classes are the TRP channels, a broad family of ion channels that have sensory functions in a range of systems (Clapham, 2003; see below). Interestingly, MA currents share a number of properties with those mediated by members of the TRP channel family. These include inhibition by low micromolar concentrations of ruthenium red (in a voltage-dependent manner similar to that observed in this study (Watanabe *et al.* 2002)) and by gadolinium, blockade by external Ca^{2+} and non-selective cation permeabilities (Drew *et al.* 2002; and see Clapham *et al.* 2001; Gunthorpe *et al.* 2002, for reviews). Although none of these properties are unique to TRP channels, the similarities are highlighted by recent observations demonstrating a central role for TRP channels in a number of mechanosensory systems. The TRP-related channel NompC is probably a transduction channel in both *Drosophila* sensory bristle cells (Walker *et al.* 2000) and zebrafish hair cells (Sidi *et al.* 2003), whilst Nanchung is crucial for *Drosophila* chordotonal neurone mechanosensation (Kim *et al.* 2003). In mammalian systems TRPV4 is activated by hypotonicity in cell lines (Liedtke *et al.* 2000; Strotmann *et al.* 2000) and probably underlies similar currents in DRG neurones (Alessandri-Haber *et al.* 2003). Thus, TRPV4 can be activated mechanically without extracellular 'anchoring', although activation is slow and there is evidence that it may be indirect and dependent on phosphorylation (Xu *et al.* 2003). TRPV4 null mutants appear to have some deficits in their responses to mechanical stimuli (Suzuki *et al.* 2003) although these authors state that only small neurones (accounting for 11% of all DRG neurones) expressed TRPV4 suggesting a limited role for this protein. Alessandri-Haber *et al.* (2003) provided evidence that this channel is activated by hypo-osmolarity in nociceptors *in vivo*. To date, no other TRP channels have clearly been implicated in mammalian sensory mechanotransduction.

The role of ASICs in mammalian mechanosensation remains to be determined. Homology between *C. elegans* MEC channels and ASICs led to the hypothesis that ASICs may function within a transduction complex in mammals (Welsh *et al.* 2002). For example, ASIC2 binds to a stomatin-like protein, Nstom1, which shows homology to MEC-2 (Eilers *et al.* 2002). Thus, mechanosensitivity may be conferred on ASICs only within the correct environment, which must include appropriate extracellular proteins. However, if ASICs are central to mechanotransduction, in contrast to *C. elegans*, much redundancy must exist between channel types: ASICs are expressed across all cell types of the DRG (Waldmann & Lazdunski, 1998; Alvarez de la Rosa *et al.* 2002) and Garcia-Añoveros *et al.* (2001) found ASIC2 immunoreactivity in all NF-200-positive peripheral sensory endings that were examined. However, mechanosensory deficits in ASIC2 and ASIC3 nulls were restricted to only two subsets of fibres in each mutant (Price *et al.* 2000, 2001) and the mechanical response properties of ASIC1 KO mice are normal (G. R. Lewin, personal communication). Moreover, altered firing rates in ASIC3 nulls were not limited to mechanoreceptors as acid- and heat-evoked activity was reduced in C-fibres (Price *et al.* 2001). Finally, despite changes in suprathreshold firing rates, neither slowly nor rapidly adapting mechanoreceptors had altered thresholds of activation in ASIC2 or ASIC3 null mutants (Price *et al.* 2000, 2001). The precise role of ASIC2 and 3 in modulating firing frequencies in response to mechanical stimulation thus remains to be determined. A simpler hypothesis is that other ion channels, such as those underlying mechanically activated currents in cultured DRG neurones, have a more primary role in mechanotransduction.

References

Alessandri-Haber N, Yeh JJ, Boyd AE, Parada CA, Chen X, Reichling DB & Levine JD (2003). Hypotonicity induces TRPV4-mediated nociception in rat. *Neuron* **39**, 497–511.

Alvarez de la Rosa D, Zhang P, Shao D, White F & Canessa CM (2002). Functional implications of the localization and activity of acid-sensitive channels in rat peripheral nervous system. *Proc Natl Acad Sci U S A* **99**, 2326–2331.

Bennett DL, Averill S, Clary DO, Priestley JV & McMahon SB (1996). Postnatal changes in the expression of the trkA high-affinity NGF receptor in primary sensory neurons. *Eur J Neurosci* **8**, 2204–2208.

Benson CJ, Xie J, Wemmie JA, Price MP, Henss JM, Welsh MJ & Snyder PM (2002). Heteromultimers of DEG/ENaC subunits form H^+-gated channels in mouse sensory neurons. *Proc Natl Acad Sci U S A* **99**, 2338–2343.

Carroll P, Lewin GR, Koltzenburg M, Toyka KV & Thoenen H (1998). A role for BDNF in mechanosensation. *Nat Neurosci* **1**, 42–46.

Cesare P & McNaughton P (1996). A novel heat-activated current in nociceptive neurons and its sensitization by bradykinin. *Proc Natl Acad Sci U S A* **93**, 15435–15439.

Chen CC, England S, Akopian AN & Wood JN (1998). A sensory neuron-specific, proton-gated ion channel. *Proc Natl Acad Sci U S A* **95**, 10240–10245.

Clapham DE (2003). TRP channels as cellular sensors. *Nature* **426**, 517–524.

Clapham DE, Runnels LW & Strubing C (2001). The TRP ion channel family. *Nat Rev Neurosci* **2**, 387–396.

Colbert HA, Smith TL & Bargmann CI (1997). OSM-9, a novel protein with structural similarity to channels, is required for olfaction, mechanosensation, and olfactory adaptation in *Caenorhabditis elegans*. *J Neurosci* **17**, 8259–8269.

Dirajlal S, Pauers LE & Stucky CL (2003). Differential response properties of IB(4)-positive and -negative unmyelinated sensory neurons to protons and capsaicin. *J Neurophysiol* **89**, 513–524.

Djouhri L, Bleazard L & Lawson SN (1998). Association of somatic action potential shape with sensory receptive properties in guinea-pig dorsal root ganglion neurones. *J Physiol* **513**, 857–872.

Drew LJ, Wood JN & Cesare P (2002). Distinct mechanosensitive properties of capsaicin-sensitive and -insensitive sensory neurons. *J Neurosci* **22**, RC228.

Eilers A, Martinez-Salgado C & Lewin GR (2002). Molecular interactions between stomatin and ASIC/DEG family proteins. *Program No. 449.7 2002 Abstract Viewer/Itinerary Planner*. Society for Neuroscience, Washington, DC.

Ernstrom GG & Chalfie M (2002). Genetics of sensory mechanotransduction. *Annu Rev Genet* **36**, 411–453.

Fitzgerald M & Fulton BP (1992). The physiological properties of developing sensory neurons. In: *Sensory Neurons. Diversity, Development, and Plasticity* (ed. SA Scott), pp. 287–306. Oxford University Press, New York.

Garcia-Añoveros J, Samad TA, Zuvela-Jelaska L, Woolf CJ & Corey DP (2001). Transport and localization of the DEG/ENaC ion channel BNaC1alpha to peripheral mechanosensory terminals of dorsal root ganglia neurons. *J Neurosci* **21**, 2678–2686.

Gillespie PG & Walker RG (2001). Molecular basis of mechanosensory transduction. *Nature* **413**, 194–202.

Gunthorpe MJ, Benham CD, Randall A & Davis JB (2002). The diversity in the vanilloid (TRPV) receptor family of ion channels. *Trends Pharmacol Sci* **23**, 183–191.

Kim J, Chung YD, Park DY, Choi S, Shin DW, Soh H, Lee HW, Son W, Yim J, Park CS, Kernan MJ & Kim C (2003). A TRPV family ion channel required for hearing in *Drosophila*. *Nature* **424**, 81–84.

Koerber HR, Druzinsky RE & Mendell LM (1988). Properties of somata of spinal dorsal root ganglion cells differ according to peripheral receptor innervated. *J Neurophysiol* **60**, 1584–1596.

Koltzenburg M, Stucky CL & Lewin GR (1997). Receptive properties of mouse sensory neurons innervating hairy skin. *J Neurophysiol* **78**, 1841–1850.

Lawson SN (2002). Phenotype and function of somatic primary afferent nociceptive neurones with C-, Aδ- or Aα/β-fibres. *Exp Physiol* **87**, 239–244.

Lewin GR & Stucky CL (2000). Sensory neuron mechanotransduction: Regulation and underlying molecular mechanisms. In *Molecular Basis of Pain Transduction*, ed. Wood JN, pp. 129–148. Wiley-Liss, New York.

Liedtke W, Choe Y, Martí-Renom MA, Bell AM, Denis CS, Ali A, Hudspeth AJ & Friedman JM (2000). Vanilloid receptor-related osmotically activated channel (VR-OAC), a candidate vertebrate osmoreceptor. *Cell* **103**, 525–535.

Molliver DC, Wright DE, Leitner ML, Parsadanian AS, Doster K, Wen D, Yan Q & Snider WD (1997). IB4-binding DRG neurons switch from NGF to GDNF dependence in early postnatal life. *Neuron* **19**, 849–861.

McCarter GC, Reichling DB & Levine JD (1999). Mechanical transduction by rat dorsal root ganglion neurons in vitro. *Neurosci Lett* **273**, 179–182.

Mansour SL, Thomas KR & Capecchi MR (1988). Disruption of the proto-oncogene int-2 in mouse embryo-derived stem cells: a general strategy for targeting mutations to non-selectable genes. *Nature* **336**, 348–352.

Nagy A, Rossant J, Nagy R, Abramow-Newerly W & Roder JC (1993). Derivation of completely cell culture-derived mice from early-passage embryonic stem cells. *Proc Natl Acad Sci U S A* **90**, 8424–8428.

Petruska JC, Napaporn J, Johnson RD, Gu JG & Cooper BY (2000). Subclassified acutely dissociated cells of rat DRG: histochemistry and patterns of capsaicin-, proton-, and ATP-activated currents. *J Neurophysiol* **84**, 2365–2379.

Price MP, Lewin GR, McIlwrath SL, Cheng C, Xie J, Heppenstall PA, Stucky CL, Mannsfeldt AG, Brennan TJ, Drummond HA, Qiao J, Benson CJ, Tarr DE, Hrstka RF, Yang B, Williamson RA & Welsh MJ (2000). The mammalian sodium channel BNC1 is required for normal touch sensation. *Nature* **407**, 1007–1011.

Price MP, McIlwrath SL, Xie J, Cheng C, Qiao J, Tarr DE, Sluka KA, Brennan TJ, Lewin GR & Welsh MJ (2001). The DRASIC cation channel contributes to the detection of cutaneous touch and acid stimuli in mice. *Neuron* **32**, 1071–1083.

Reid G, Babes A & Pluteanu F (2002). A cold- and menthol-activated current in rat dorsal root ganglion neurones: properties and role in cold transduction. *J Physiol* **545**, 595–614.

Ritter AM & Mendell LM (1992). Somal membrane properties of physiologically identified sensory neurons in the rat: effects of nerve growth factor. *J Neurophysiol* **68**, 2033–2041.

Rose RD, Koerber HR, Sedivec MJ & Mendell LM (1986). Somal action potential duration differs in identified primary afferents. *Neurosci Lett* **63**, 259–264.

Sidi S, Friedrich RW & Nicolson T (2003). NompC TRP channel required for vertebrate sensory hair cell mechanotransduction. *Science* **301**, 96–99.

Strotmann R, Harteneck C, Nunnenmacher K, Schultz G & Plant TD (2000). OTRPC4, a nonselective cation channel that confers sensitivity to extracellular osmolarity. *Nat Cell Biol* **2**, 695–702.

Stucky CL & Lewin GR (1999). Isolectin B(4)-positive and -negative nociceptors are functionally distinct. *J Neurosci* **19**, 6497–6505.

Stucky CL, Rossi J, Airaksinen MS & Lewin GR (2002). GFR alpha2/neurturin signalling regulates noxious heat transduction in isolectin B4-binding mouse sensory neurons. *J Physiol* **545**, 43–50.

Suzuki M, Mizuno A, Kodaira K & Imai M (2003). Impaired pressure sensation in mice lacking TRPV4. *J Biol Chem* **278**, 22664–22668.

Tavernarakis N & Driscoll M (1997). Molecular modeling of mechanotransduction in the nematode *Caenorhabditis elegans*. *Annu Rev Physiol* **59**, 659–689.

Waldmann R, Champigny G, Bassilana F, Heurteaux C & Lazdunski M (1997). A proton-gated cation channel involved in acid-sensing. *Nature* **386**, 173–177.

Waldmann R & Lazdunski M (1998). H^+-gated cation channels: neuronal acid sensors in the NaC/DEG family of ion channels. *Curr Opin Neurobiol* **8**, 418–424.

Walker RG, Willingham AT & Zuker CS (2000). A *Drosophila* mechanosensory transduction channel. *Science* **287**, 2229–2234.

Watanabe H, Davis JB, Smart D, Jerman JC, Smith GD, Hayes P, Vriens J, Cairns W, Wissenbach U, Prenen J, Flockerzi V, Droogmans G, Benham CD & Nilius B (2002). Activation of TRPV4 channels (hVRL-2/mTRP12) by phorbol derivatives. *J Biol Chem* **277**, 13569–13577.

Welsh MJ, Price MP & Xie J (2002). Biochemical basis of touch perception: mechanosensory function of degenerin/epithelial Na^+ channels. *J Biol Chem* **277**, 2369–2372.

Xie J, Price MP, Berger AL & Welsh MJ (2002). DRASIC contributes to pH-gated currents in large dorsal root ganglion sensory neurons by forming heteromultimeric channels. *J Neurophysiol* **87**, 2835–2843.

Xu H, Zhao H, Tian W, Yoshida K, Roullet JB & Cohen DM (2003). Regulation of a transient receptor potential (TRP) channel by tyrosine phosphorylation. SRC family kinase-dependent tyrosine phosphorylation of TRPV4 on TYR-253 mediates its response to hypotonic stress. *J Biol Chem* **278**, 11520–11527.

Acknowledgements

We would like to thank Mark Baker for his advice and comments on the manuscript and Michael Welsh for the provision of ASIC2 null mice. The Wellcome Trust and MRC supported this work.

Authors' present addresses

P. Cesare: Dip. di Biologia Cellulare e dello Sviluppo, Universitá degli Studi di Roma 'La Sapienza', Piazzale Aldo Moro 5, 00185 Roma, Italy.

D. K. Rohrer: Medarex, Inc., 521 Cottonwood Drive, Milpitas, CA 95035, USA.

Supplementary material

The online version of this paper can be found at:
DOI: 10.1113/jphysiol.2003.058693
and contains supplementary material consisting of a table (Table A) entitled: Physiological properties of neurones defined by their genotype, size and their response to mechanical stimulation.
This material is also available at http://www.blackwellpublishing.com/products/journals/suppmat/tjp/tjp220/tjp220sm.htm